Journal of Atmospheric and Solar-Terrestrial Physics 71 (2009) 653–661

Contents lists available at ScienceDirect

Journal of
Atmospheric and Solar-Terrestrial Physics

journal homepage: www.elsevier.com/locate/jastp

Latitudinal and seasonal variability of the micrometeor input function: A study using model predictions and observations from Arecibo and PFISR

J.T. Fentzke [a,b,*], D. Janches [b], J.J. Sparks [b,c]

[a] Department of Aerospace Engineering, University of Colorado, Boulder, CO 80301, USA
[b] NorthWest Research Associates Inc., CoRA Division, 3380 Mitchell Lane, Boulder, CO 80301, USA
[c] Department of Physics, University of Colorado, Boulder, CO 80301, USA

ARTICLE INFO

Article history:
Accepted 22 July 2008
Available online 5 August 2008

Keywords:
Meteors
Radar
Modeling
Mesosphere and lower thermosphere

ABSTRACT

In this work, we use a semi-empirical model of the micrometeor input function (MIF) together with meteor head-echo observations obtained with two high power and large aperture (HPLA) radars, the 430 MHz Arecibo Observatory (AO) radar in Puerto Rico (18°N, 67°W) and the 450 MHz Poker flat incoherent scatter radar (PFISR) in Alaska (65°N, 147°W), to study the seasonal and geographical dependence of the meteoric flux in the upper atmosphere. The model, recently developed by Janches et al. [2006a. Modeling the global micrometeor input function in the upper atmosphere observed by high power and large aperture radars. Journal of Geophysical Research 111] and Fentzke and Janches [2008. A semi-empirical model of the contribution from sporadic meteoroid sources on the meteor input function observed at arecibo. Journal of Geophysical Research (Space Physics) 113 (A03304)], includes an initial mass flux that is provided by the six known meteor sources (i.e. orbital families of dust) as well as detailed modeling of meteoroid atmospheric entry and ablation physics. In addition, we use a simple ionization model to treat radar sensitivity issues by defining minimum electron volume density production thresholds required in the meteor head-echo plasma for detection. This simplified approach works well because we use observations from two radars with similar frequencies, but different sensitivities and locations. This methodology allows us to explore the initial input of particles and how it manifests in different parts of the MLT as observed by these instruments without the need to invoke more sophisticated plasma models, which are under current development. The comparisons between model predictions and radar observations show excellent agreement between diurnal, seasonal, and latitudinal variability of the detected meteor rate and radial velocity distributions, allowing us to understand how individual meteoroid populations contribute to the overall flux at a particular location and season.

1. Introduction

Accurate knowledge of the meteoric input function (MIF) is a necessary prerequisite for a thorough understanding of atmospheric phenomena observed in the mesosphere and lower thermosphere (MLT) related to micrometeoric ablated material (i.e. metallic layers, noctilucent clouds, meteoric smoke, etc.). These parameters include annual, diurnal and geographical variations of meteor rate, global and local mass flux, directionality, and velocity distributions. Although each system is sensitive to a somewhat different mass range, high power and large aperture (HPLA) radars offer an excellent means to study the most abundant meteor flux contributions by sub-millimeter particles (Janches et al., 2000, 2008). This flux originates mostly from the sporadic meteor background as opposed to isolated less frequent meteor showers (Ceplecha et al., 1998; Baggaley, 2002; Williams and Murad, 2002).

Previous modeling attempts to quantify meteoric flux contributions to the MLT (~100 km) phenomena tend to misrepresent or oversimplify the characteristics of the MIF even though observations show that these are highly variable depending on season and geographical location (Plane, 2004; Singer et al., 2004; Janches et al., 2004b, 2006; Fentzke and Janches, 2008; Sparks et al., 2008). The misrepresentation is generally due to the fact that most aeronomical models rarely consider the directionality of the incoming flux and adopt a constant average incoming entry angle as if the sporadic meteoroid radiant distribution is isotropic (McNeil et al., 1998, 2002; Plane, 2004; Pesnell et al., 2004; Megner et al., 2006), which is not representative of the observed meteoric flux (Jones and Brown, 1993; Galligan and

* Corresponding author at: Department of Aerospace Engineering, University of Colorado, Boulder, CO 80301, USA. Tel.: +1 716 4817475.
E-mail addresses: jonathan.fentzke@colorado.edu (J.T. Fentzke), diego@cora.nwra.com (D. Janches), jonathan.sparks@colorado.edu (J.J. Sparks).

1364-6826/$ - see front matter © 2008 Elsevier Ltd. All rights reserved.
doi:10.1016/j.jastp.2008.07.015

Baggaley, 2005). In the same manner models tend to misrepresent the geocentric velocity distribution of the incoming meteoric mass by either using a single low value (Plane, 1991; Love and Brownlee, 1991; McNeil et al., 1995) or by considering a range of only slow particles between 15 and 25 km/s (Hunten et al., 1980; Pesnell et al., 2004; Megner et al., 2006) unless a particular meteor shower is being modeled.

As noted by Ceplecha et al. (1998), the main contribution of meteors in the earth's atmosphere comes from sporadic meteoroids, that is, particles not associated with a particular known shower. These sporadic meteoroids originate from six known radiant distributions (i.e. orbital families), which are the North and South Apex, composed mainly of dust from long period comets; the Helion and anti-Helion, composed of dust from short period comets; and the North and South Toroidal composed of dust from Halley-family type comets with the radiants near the ecliptic poles being from asteroidal sources (Jones and Brown, 1993; Taylor, 1997; Taylor and Elford, 1998). The fact that meteors come from specific regions in the sky in a heliocentric frame of reference translates into a very specific set of incoming directions in a geocentric frame of reference that highly depend on time of day, season, and geographical location. For example, while a particular radiant source can be high in the local sky near the equator, it will be below the horizon at other geographical locations. This type of variability will be accentuated at polar latitudes as shown by Janches et al. (2006).

Recently, Janches et al. (2006) and Fentzke and Janches (2008) developed a semi-empirical model to simulate the seasonal characteristics of the MIF observed with the Arecibo 430 MHz radar in Puerto Rico (18°N, 66°W). This model considers the astronomical characteristics of these sources as well as the physical processes that each meteoroid undergoes during their atmospheric entry. In order to understand how much, when and where micrometeor mass is deposited in the Earth's atmosphere, we investigate here how these different meteoroid populations contribute to the local diurnal and seasonal meteor rates at high latitudes using meteor head-echo observations performed with the new 450 MHz Poker Flat Incoherent Scatter Radar (PFISR) in Alaska (65°N, 147°W). Furthermore, we compare these results with those from Arecibo (Fentzke and Janches, 2008) in order to show that different meteoroid sources from a single global mass flux are responsible for producing distinct diurnal and seasonal variability in the observed meteor flux at equatorial and northern latitudes and thus providing very different local inputs.

The details of our modeled canonical meteoroid physics and parameters are discussed in Fentzke and Janches (2008). The Arecibo observations are described in Janches et al. (2003) while the observations obtained with PFISR are presented in a companion paper reported by Sparks et al. (2008). In both cases, we pointed the radar beam vertically, thus the resulting measured radial velocities are the vertical component of the absolute meteoroid speed. As discussed by Janches et al. (2008), each HPLA radar must be treated as a unique instrument because their sensitivity will strongly depend on its aperture as well as power and frequency transmitted. Since both radars used in this work utilize very similar frequencies, assumptions on the detection of the head-echo plasma as a function of the transmitted wavelength can be made, simplifying our present efforts. However, sensitivity considerations due to differences in aperture need to be made. This is presented in Section 2. Ultimately a more thorough treatment of the meteor radar cross section (RCS) is necessary and is under current development (Dyrud et al., 2007; Dyrud and Janches, 2008). Comparisons and discussions between modeled and observed results at PFISR and Arecibo are presented in Section 3 and our conclusions are discussed in Section 4. This effort is intended to provide a better estimate of the amount and associated properties of meteoric material that will be deposited on a given small volume placed on the MLT at a particular time, given a known extraterrestrial flux and geographical location.

2. Modeling PFISR observations

As discussed in Fentzke and Janches (2008) our MIF model uses a Monte Carlo simulation in order to predict observable HPLA radar parameters, such as particle flux and radial velocity distributions, with the goal of determining the micrometeoric mass flux within a small volume placed on the MLT at any location on Earth as a function of time and season. By assuming an initial global mass input above Earth's atmosphere (Ceplecha et al., 1998) and considering the properties of the six main sporadic meteoroid populations (Jones and Brown, 1993; Taylor, 1997; Taylor and Elford, 1998; Galligan and Baggaley, 2005) (see Table 1 for a summary of pertinent parameters) it is possible to determine the time evolution of the sporadic meteoroid populations' incoming angular and velocity characteristics in a given geographical location. We then use an ablation and ionization model based on the canonical meteor equations (Whipple, 1950, 1951; McKinley, 1961; Bronshten, 1983) to determine radar detectability. A flow chart summarizing the current status of our model is displayed in Fig. 1.

Currently the main instrumental parameters needed in our model are the geographic location of the radar, the effective beam size and the sensitivity to head-echo detections. In Fentzke and Janches (2008) the focus was simulating meteor head-echo observations obtained with the Arecibo radar. For that work, we assumed the illuminated volume in the MLT to be in Arecibo's antenna near-field and thus considered the beam to be a uniform cylinder with a diameter of ~400 m. This included the first ring lobe where meteors are consistently detected (Janches et al., 2004a; Dyrud and Janches, 2008). For the case of PFISR's observations, since its aperture is smaller but the transmitted frequency is similar, this translates into a wider radar beam and

Table 1
Gaussian fitting parameterization of radiant source distribution

Source name	Geocentric velocity distribution						Sun centered location		Sun centered width	
	$A_\circ$		$\overline{V}$ (km/s)		σ (km/s)					
	Fast part	Slow part	Fast part	Slow part	Fast part	Slow part	$\overline{\lambda}$ (deg.)	$\overline{\sigma}$ (deg.)	σ_λ (deg.)	σ_β (deg.)
Apex	0.8	0.2	55	17.3	2.5	2.60	270	0	19	32
Helion		1.0		30.0		2.57	350	0	8	20
Anti-Helion		1.0		30.0		2.57	190	0	8	20
North Toroidal		1.0		30.0		2.57	270	60	17	17
South Toroidal		1.0		30.0		2.57	270	−60	17	17

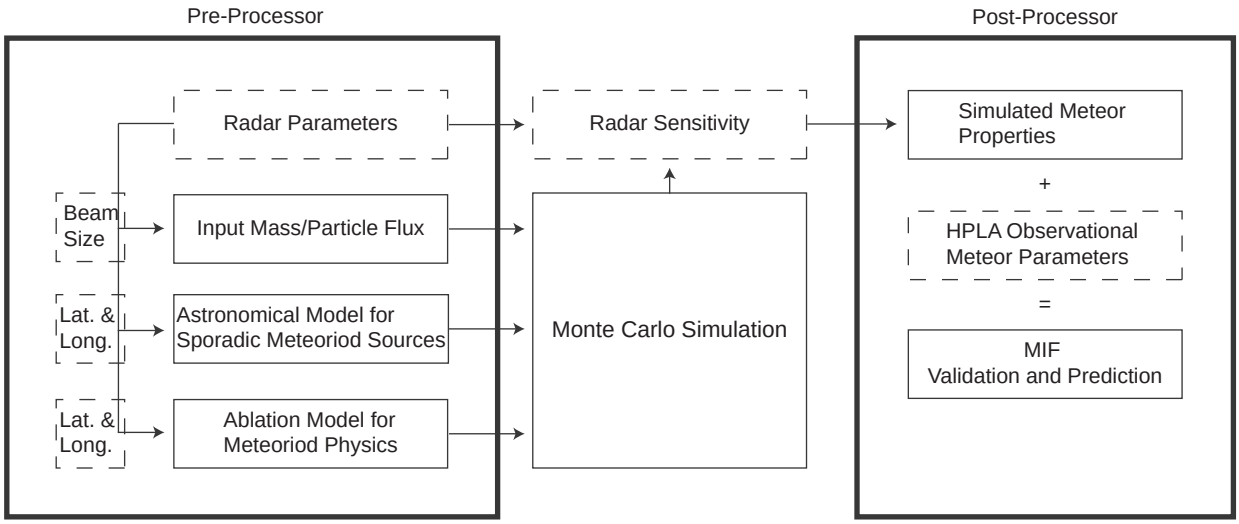

Fig. 1. Block diagram of model.

lower sensitivity as the observed results suggest (Sparks et al., 2008). Thus, we assume an effective beam size with a diameter approximately seven times larger than the Arecibo beam (~2800 m; Heinselman and Nicolls, 2008, personal communication) that represents a physical approximation of the more sensitive portion of the PFISR main beam (>35 dB).

An additional consideration that is necessary for each radar is the sensitivity to a particular meteoroid mass and velocity range, since Janches et al. (2008) showed that these can be very different depending on the HPLA radar utilized. For the case of the Arecibo radar, Fentzke and Janches (2008) argued that as long as the particle size is above the limit of ablation reported by Bronshten (1983), the majority of meteors should produce enough electrons to be detected by the radar independent of velocity. However, because of the lower PFISR sensitivity due to its smaller aperture compared to that of Arecibo, these mass and velocity biases must be reformulated. In this work, we treat this detection issue utilizing the RCS model developed by Close et al. (2005), used to provide a first estimation of the mass–velocity bias of a particular system. This is done in a way similar to Close et al. (2007) for the case of the ALTAIR VHF (160 MHz) radar and Janches et al. (2008) to interpret the Arecibo observations. In particular the latter, using this spherical plasma scattering model, confirmed the findings of Fentzke and Janches (2008) in terms of the lack of mass–velocity biases in this highly sensitive radar for particles with sizes above the limit of ablation (Bronshten, 1983). Fig. 2 displays the estimated detected RCS for both, Arecibo and PFISR, derived assuming spherical targets as described by Janches et al. (2008). From this figure it can be seen that while Arecibo seems to be sensitive to particles with RCS as low as ~ -93 dBsm, PFISR's detected minimum RCS is estimated to be ~ -65 dBsm. It is important to note that these RCS limits are likely to be overestimated (Janches et al., 2008). Since the PFISR's transmitted frequency is essentially the same as Arecibo, we can move the detection threshold set at Arecibo's sensitivity in Fig. 2b of Janches et al. (2008) up to that of PFISR and thus have a first guess of the mass–velocity bias present in PFISR's observations. We used this methodology to selectively remove particles according to their mass and velocity based on RCS, according to the model results presented in Janches et al. (2008), which will be below PFISR's detectability threshold.

We note that this is a simplistic view of a complicated process and a more thorough treatment is under current development, which includes the parameterization of thousands of finite

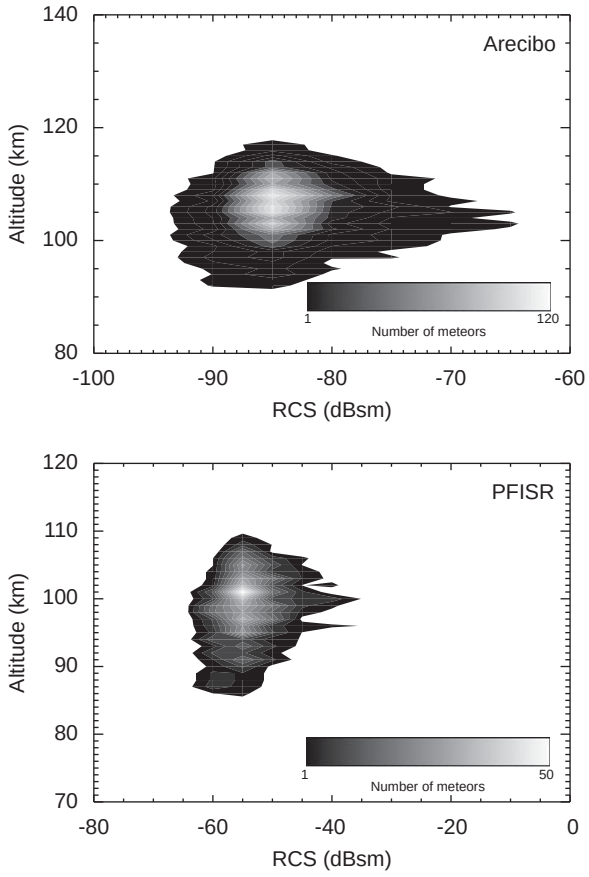

Fig. 2. Observed RCS assuming spherical targets as described by Janches et al. (2008).

difference time domain (FDTD) simulations of electromagnetic waves interacting with the head-echo plasma (Dyrud et al., 2007; Dyrud and Janches, 2008). Finally, we note in Fig. 2 that the detected RCS for PFISR reach much higher values than Arecibo. In theory, because Arecibo is more sensitive than PFISR, it should be able to detect meteors with RCS as large as those detected by PFISR. We argue however that, for a given entry angle and velocity, larger values of RCS are likely produced by larger particles, which

are less frequent (Ceplecha et al., 1998). Thus, the lack of these larger RCS values in Arecibo's observations is most likely due to its much smaller collecting volume making it statistically unlikely to detect these larger particles. This is in agreement with the fact that the PFISR observed meteor altitude distributions are significantly lower than those obtained with Arecibo (Janches et al., 2003; Sparks et al., 2008), which indicates that larger particles need to penetrate lower into the MLT before being detected by PFISR. This is shown in Fig. 3 where a comparison between our modeled and observed detected meteor initial altitude (Janches and ReVelle, 2005) as a function of velocity is presented for both, the Arecibo and PFISR observations. This observational data is used, at present, to calibrate the appropriate electron threshold used in the model as a simplified sensitivity proxy to determine if and when meteors are observed by the radars (Fentzke and Janches, 2008). The modeled results in this figure represent the altitude at which the meteor, given its velocity, mass and entry angle, reached the chosen minimum electron volume density estimated by the ablation module. As explained in Fentzke and Janches (2008), this electron density value is used as the threshold for detectability. The values of these thresholds are 1×10^8 and 1×10^{14} e^-/m^3 for Arecibo and PFISR, respectively. This threshold together with the RCS model implies that if the particle mass is greater than 10^{-3} μg for Arecibo and 10^1 μg for PFISR the meteor will be detected independent of its velocity. These values are utilized hereafter for all seasons and results are presented below.

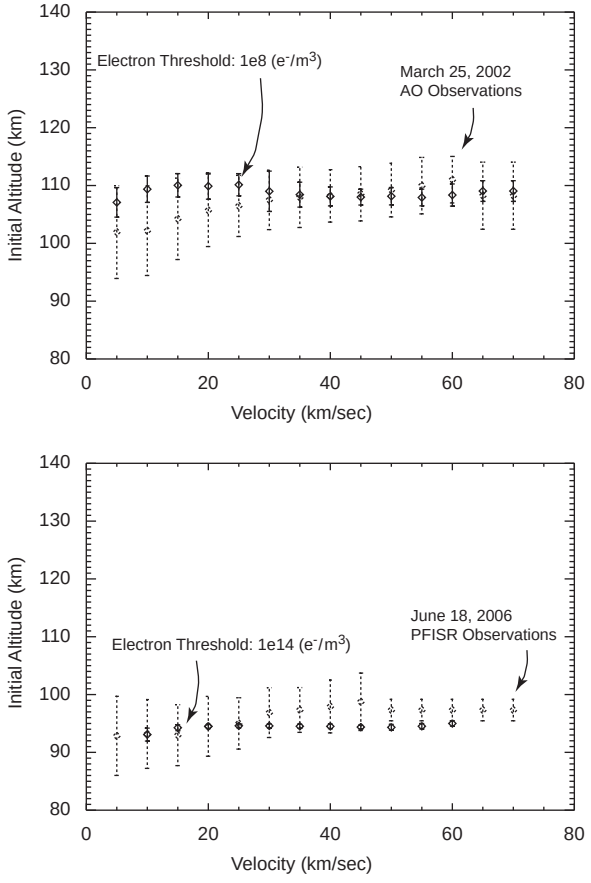

Fig. 3. Observational and model comparison of initial altitude of detection as a function of velocity with 5 km/s binning. The dotted diamonds with 1 standard deviation error bars are (a) Arecibo observations obtained on March 25, 2002, and (b) PFISR observations obtained on June 18, 2006. The solid diamonds with 1 standard deviation error bars are modeled results assuming (a) $e^-_{\text{threshold}}$ of 1×10^8 e^-/m^3, and (b) $e^-_{\text{threshold}}$ of 1×10^{14} e^-/m^3.

3. Seasonal and latitudinal variability: results and discussions

Most of the previous modeling work on the MIF as observed by HPLA radars has been focused on the Arecibo radar, due to the wealth of available data (Janches et al., 2003, 2006; Janches and Chau, 2005; Fentzke and Janches, 2008). In addition, several works have investigated limitedly the MIF at high latitudes using observations by the HPLA radars at Sanderstrom, Greenland (67°N, 51°W) (Janches et al., 2006) and the UHF and VHF EISCAT system in northern Scandinavia (~69°N, ~20°E (Westman et al., 2004). Previous work by Janches et al. (2004b) and Singer et al. (2004) showed an asymmetrical distribution in the flux derived from meteor trail-echos using specular meteor radars (SMRs) at both poles. Later, Janches et al. (2006) modeled this asymmetry for different HPLA radars and showed that the seasonal variability of the MIF becomes more pronounced with increasing latitude. Recently, the PFISR HPLA radar was utilized to perform the first complete seasonal observations of meteor head-echoes at high latitudes providing the necessary data to investigate in detail the MIF in the polar MLT (Sparks et al., 2008).

Fig. 4 shows the observed and modeled fluxes at different seasons for PFISR and Arecibo. Even though the modeled beam radius of PFISR is approximately a factor of seven times larger than AO, the PFISR flux results must be binned per 20 min to provide similar count rates to those of Arecibo, which are binned at only 1 min. This is because as discussed in the previous section, PFISR is less sensitive than Arecibo. This is due to the fact that PFISR transmits similar peak power as AO, but over a larger beam width due to its smaller aperture. The lower transmitted power density at MLT altitudes implies that for a given set of entry parameters (i.e. angle and velocity) only larger meteoroids will produce enough ionization to be observed by PFISR relative to Arecibo. We can see that our model results do reproduce fairly accurately the detected flux rates, including the number of meteors per time bin detected by both radars. We note that these model rates do not have any additional normalizing factor.

Although both PFISR and AO flux results show a peak in flux near 6 am LT the diurnal curves show different shapes that are due to the observing geometry of the sporadic meteoroid sources in the local sky and the sensitivity of each radar. At PFISR the fluxes peak between 5 and 10 am LT depending on season. In particular, the September fluxes, and to a lesser degree the March fluxes at PFISR show a slight indication of a dual peak, which is very prominent in the Arecibo observed fluxes. AO shows a similar diurnal variability, however there is a distinct change in the shape of the observed and modeled flux from a single broad peak in March to a double peak in the remainder of the months shown in the lower panels of Fig. 4.

In previous modeling work (Janches et al., 2006; Fentzke and Janches, 2008), we showed that much of the velocity and flux diurnal and seasonal variations are attributed to the observing geometry of the sporadic meteor sources in the local coordinate frame of reference. Fig. 5 shows the modeled individual source contributions observed by PFISR and AO. This plot shows the capability of our model to provide statistical information on the individual contribution from each meteoroid population to the overall detected flux rates without the aid of interferometry capabilities, an observing feature that most HPLA radars do not have. As mentioned earlier, the model reproduces the observed fluxes in all seasons using the same sporadic meteoroid population parameters as input to multiple and independent radar observations.

Fig. 6 shows the PFISR (dotted lines) and AO (solid lines) radar beam paths for all the seasons projected in the ecliptic plane. This figure is in the sun-centered coordinate frame of reference (the relative motion of the earth is removed) where 0° indicates

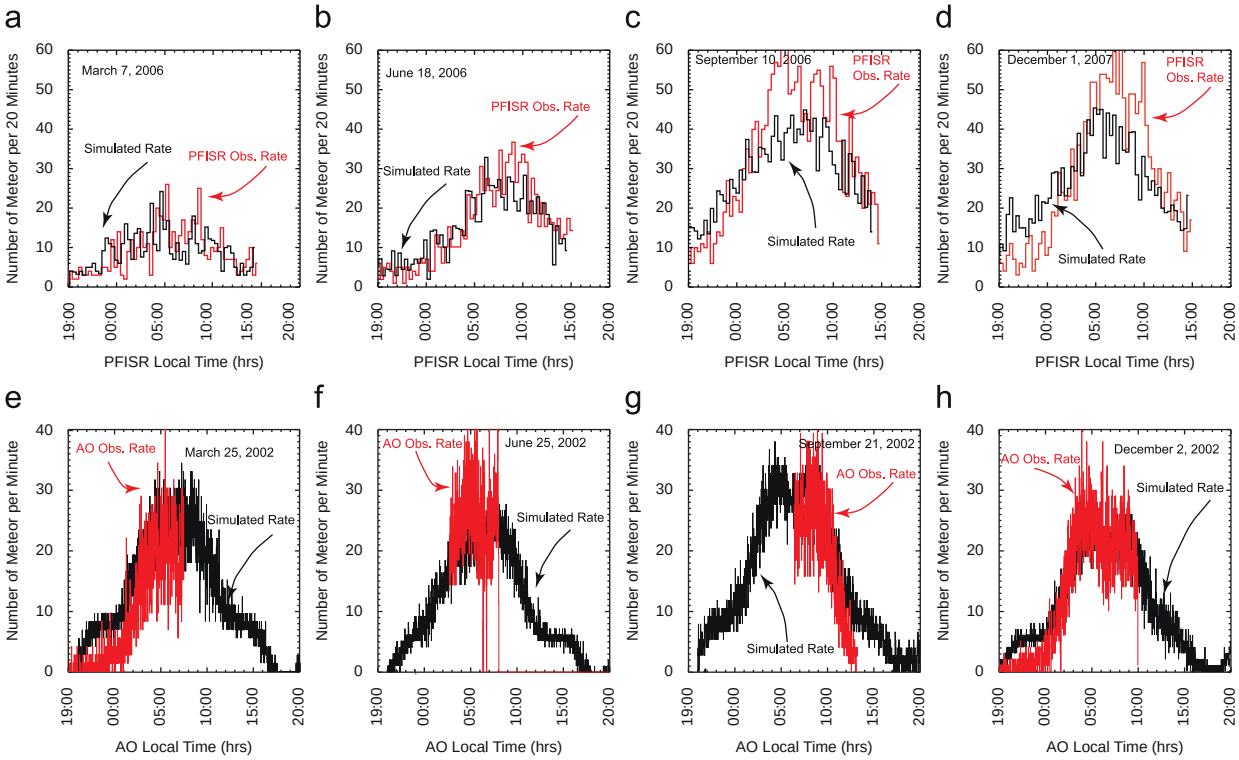

Fig. 4. (a) PFISR March flux; (b) PFISR June flux; (c) PFISR September flux; (d) PFISR December flux; (e) AO March flux; (f) AO June flux; (g) AO September flux; (h) AO December flux.

local noon and the position of antihelion at 180° indicates local midnight. The location of the six sporadic meteoroid sources is also displayed in this figure. The relative position of the beam paths with respect to the sources explains the change in large-scale features of the observed meteor rates with season. In September the PFISR radar beam scans directly through the Apex source, which is dominated by higher geocentric speed particles (~55 km/s). These higher speed particles will have, on average, entry angles closer to vertical in September, thus the increase in meteor flux (Janches et al., 2006; Sparks et al., 2008) and are more readily observed by PFISR due to the selection effect discussed in the previous section. In addition, we expected to observe a sharp decrease in the meteor flux for December relative to September, similar in magnitude to the differences observed between the June and September observations. However, as can be observed in Fig. 4, the maximum rates representative of the winter period are similar to those reached in the Fall. The reason for this is that, the December observations were taken 3 weeks before the winter solstice (Sparks et al., 2008) and according to our model (Janches et al., 2006) at this time, the meteor flux should not decrease significantly although the shape of the peak in the meteor flux as a function of time should become narrower as the observations show. This shows how drastic the seasonal and monthly differences at the polar MLT can be, that is the observed meteor flux can decrease more than 30% in a 3 weeks period. At a lower latitude, on the other hand, the Arecibo radar path variation is less severe with respect to the Apex source in different seasons (see Fig. 6). While the Apex provides the majority of counts in all seasons, the small-scale variability in the meteor flux is due to the changing observing geometry of the Helion and Anti-Helion sources (Janches et al., 2006; Fentzke and Janches, 2008). Those sources are responsible for the distinct double peak shape in the meteor flux as a function of time.

The modeled seasonal and latitudinal local contributions of the individual sources are summarized in Tables 2 and 3. These tables provide the modeled average, minimum, and maximum percentage of the observed sporadic meteoroid sources by PFISR and AO. Although the radars have different geographical locations and sensitivities, both seem to observe the majority of particles from the Apex source. Even though the Apex source is required to provide 33% of incoming particles outside Earth's atmosphere it accounts for ~55% on average of the particles seen by both PFISR and AO in the MLT. For the case of Arecibo, this is due to the fact that the faster particles from the Apex with masses less than 10^{-3} μg are more likely to ablate and produce enough ionization to be detected, unlike the slower particles from the other sources, according to Bronshten (1983). In addition, as the particle size decreases, it becomes more abundant in accordance with Ceplecha et al. (1998). The sum of both the effects result in the observed meteor flux rates and faster velocity distributions at Arecibo. In the same manner and due to the lower modeled sensitivity of PFISR, slower particles from the non-Apex sources with masses less than ~10 μg are less likely detected. Thus, PFISR modeled meteor flux and velocity distributions are dominated by particles with velocities characteristic of the Apex in the mass range of 1–10 μg. These results are based on the ablation, geometric, and plasma scattering arguments discussed earlier.

Understanding the seasonal variability of the MIF at high latitudes is crucial to determine the relationship between incoming meteor flux and atmospheric phenomena observed in the polar MLT. It is evident from Fig. 4 that the seasonal variability of the meteoric flux is more pronounced in the polar MLT where the differences between the Autumn and Spring seasons are over 50% while they are only ~15% at tropical latitudes. This is represented in more detail in Fig. 7 where the dotted line shows the modeled particle flux variation that would be observed by

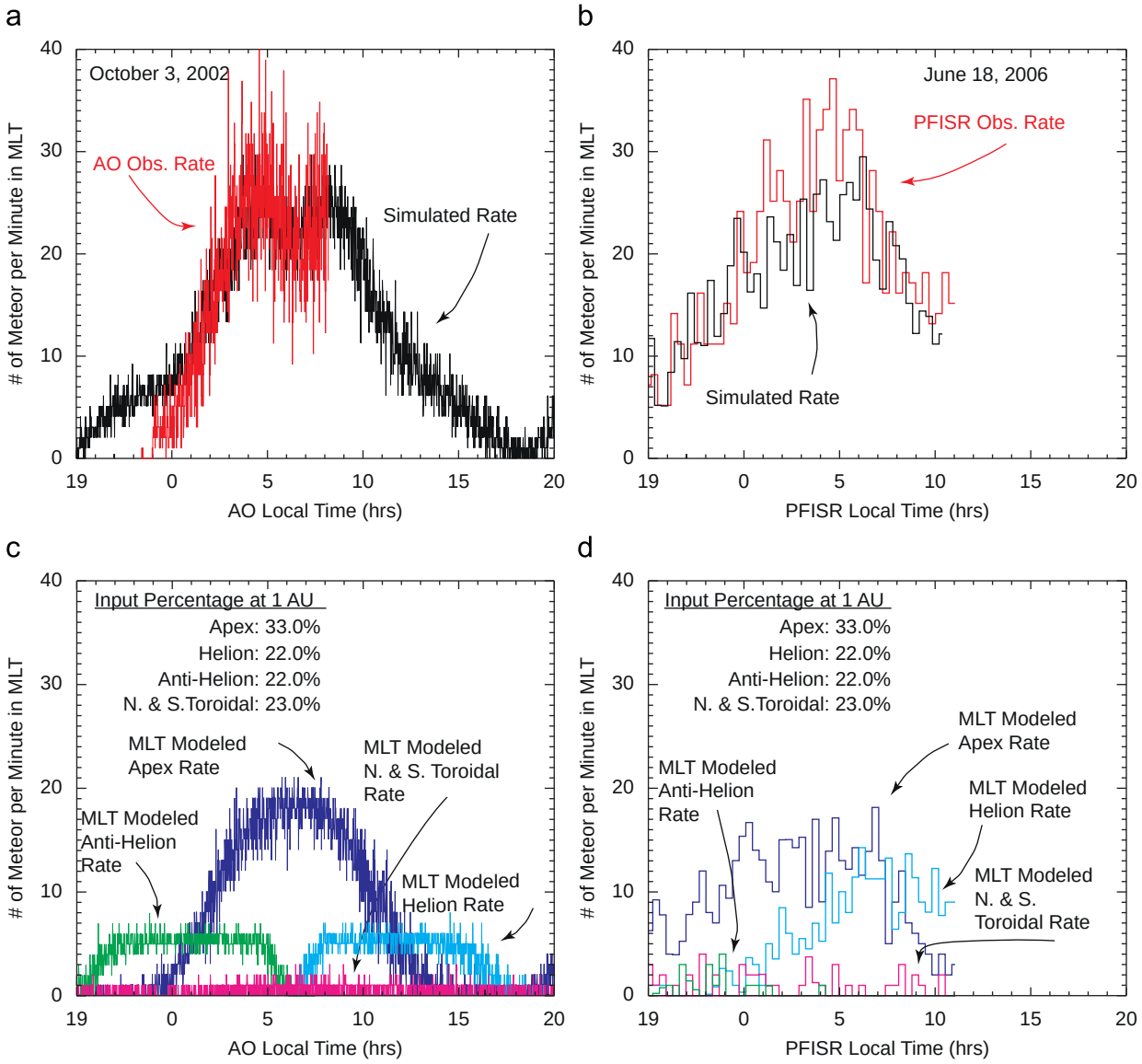

Fig. 5. (a) The total diurnal variation of observed and simulated meteor events per minute for October 2–3, 2002 at Arecibo. (b) The total diurnal variation of observed and simulated meteor events per minute for June 18, 2006 for PFISR. (c) and (d) The simulated event rates in the MLT input from each individual source. The sum of the curves in the bottom panels result in the modeled curves in the upper panels. The modeled source intensities shown in the bottom panels remain the same in both (c) and (d). However, the modeled contribution of each source to the overall MLT flux is in a much different proportion than the source contributions originating outside earth's atmosphere.

PFISR for an entire year. PFISR observations from the different seasons are shown as overlaid triangles. The model and observations are in good agreement early in the year however the September and December observations resulted in larger rates than predicted. This is probably due to the fact that our model assumes the global flux to be constant and uniform along the year and these results may indicate otherwise. Also there may be additional instrumental considerations at PFISR, not accounted for yet, by the model. It is important to note that the increase in meteoric particle flux in the summer months could have implications for meteoric smoke input, which is believed to play a crucial role in the formation of noctilucent clouds (NLC) and polar mesospheric summer echoes (PMSE).

Finally, we investigate the seasonal changes in the observed radial velocity distributions at both latitudes displayed in Fig. 8. The top panels of this figure shows a comparison between the observed and MIF modeled radial velocities at PFISR for all the seasons while the lower panels display those at Arecibo. Note that currently, we have not yet analyzed the data for Arecibo in the Fall and Winter and thus we show only the modeled results in those periods. Referring to Fig. 8 there is a distinct seasonal change in the distribution that is more pronounced at high latitudes. The peak of the distributions changes from ~20 km/s in March to almost 50 km/s in September. As discussed in Sparks et al. (2008) this is due to the fact that the observed flux is largely anisotropic and in Spring the majority of the meteor radiant elevation angles are closer to the horizon than in the Fall given the astronomical and geometrical arguments discussed here. A lower elevation implies that the meteoroids will cross the radar beam with larger horizontal velocity components and thus the radial (i.e. line-of-sight) component, which in this case is also the vertical velocity, will be lower. Once again, it is evident from this figure that our MIF model reproduces with high fidelity independent observations from two radars with similar

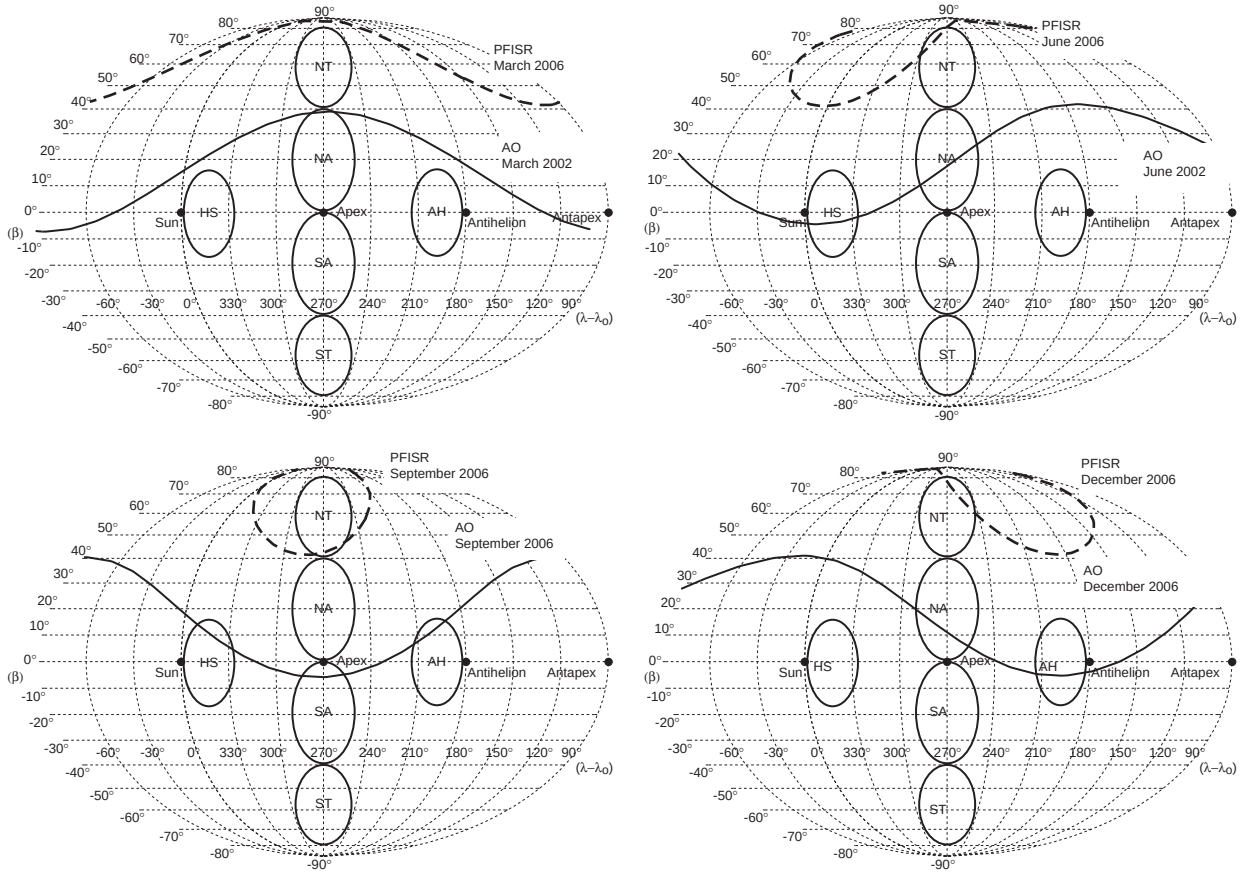

Fig. 6. (a) March; (b) June; (c) September; (d) December; (dotted lines) PFISR, (solid lines) AO.

Table 2
Average annual observed source contributions above PFISR

Source name	Model input (%) (1 AU)	Model avg. (%) (MLT)	Yearly min (%) (MLT)	Yearly max (%) (MLT)
Combined N. & S. Apex	33.0	55.33	43.74	69.16
Helion	22.0	17.88	1.84	41.19
Anti-Helion	22.0	19.17	3.30	41.14
North Toroidal	11.5	7.35	4.63	10.34
South Toroidal	11.5	0.26	0.00	0.62

Table 3
Average annual modeled source contributions above Arecibo

Source name	Model input (%) (1 AU)	Model avg. (%) (MLT)	Yearly min (%) (MLT)	Yearly max (%) (MLT)
Combined N. & S. Apex	33.0	56.17	49.93	58.85
Helion	22.0	19.26	15.15	23.43
Anti-Helion	22.0	19.44	15.13	23.43
North Toroidal	11.5	4.32	3.65	4.98
South Toroidal	11.5	1.16	0.25	2.05

transmitted frequency, but very different geographical location and sensitivity.

4. Conclusion

In this paper, we have presented meteor head-echo observations obtained with two independent HPLA radar systems and compared them with a recently developed model of the MIF (Janches et al., 2006; Fentzke and Janches, 2008). The observations were performed with the Arecibo radar in Puerto Rico and the PFISR system in Alaska. We have shown that with the same parameterization of the global micrometeoroid mass flux into the upper atmosphere, together with a redistribution of this flux into the six known sporadic sources we can model accurately the diurnal, seasonal and geographical variability of the local flux and its associated properties. That is the flux occurring at a particular geographical location given a time of the day and year. As argued in previous work (Janches et al., 2006), we have demonstrated that the relative location of the meteoroid sources in the local sky largely explain the seasonal and latitudinal differences in the observed MIF parameters.

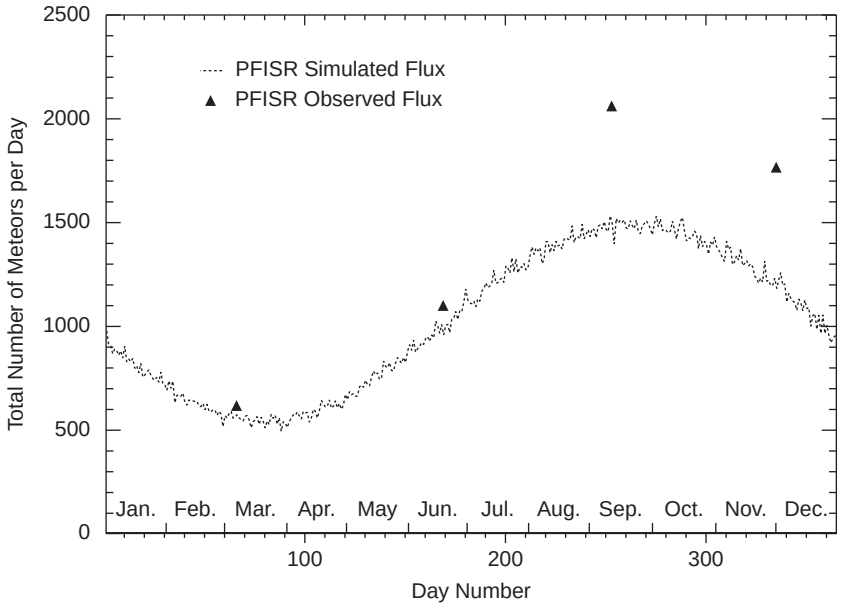

Fig. 7. Simulated particle flux variation at PFISR (dotted line) throughout the year with PFISR observations (solid triangles) from different seasons superimposed.

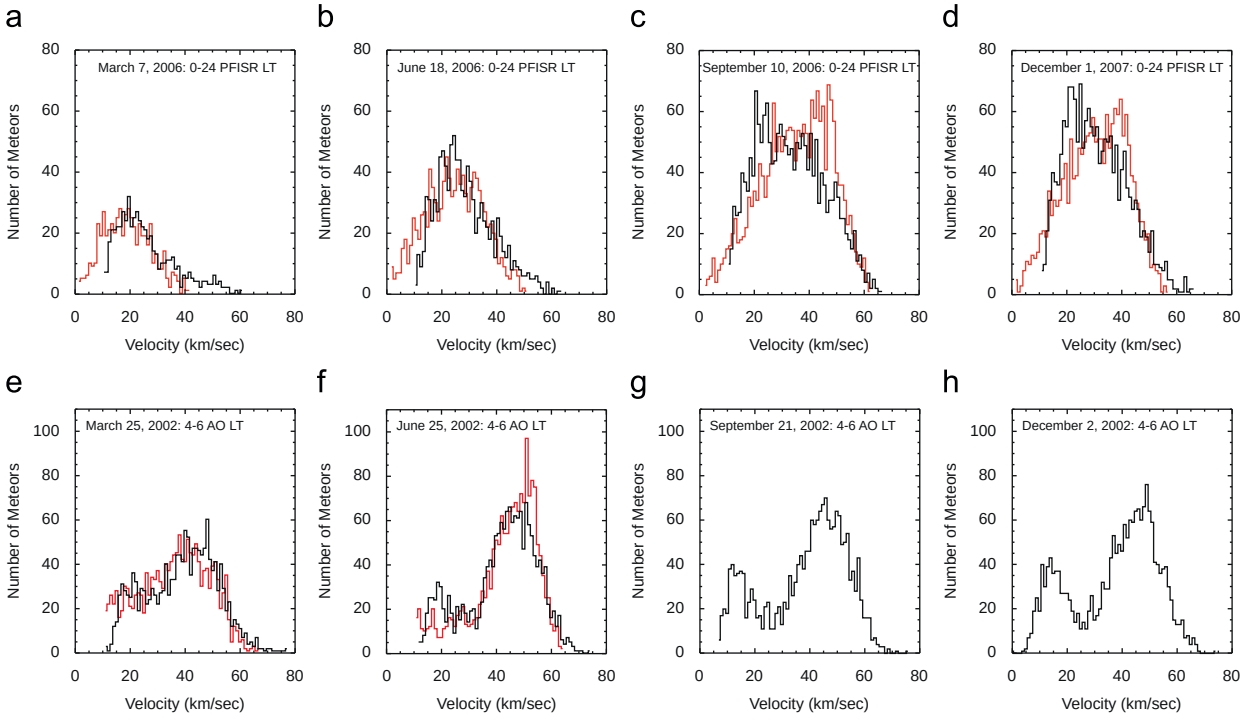

Fig. 8. PFISR radial velocity for (a) March; (b) June; (c) September; (d) December; red-observed, black-modeled. And AO radial velocity for (a) March; (b) June; (c) September; (d) December; (red) observed, (black) modeled.

In addition, since both systems transmit at almost identical frequencies, we have been able to use a simple treatment of the meteor RCS to account for the different sensitivities due to the different radar apertures. The majority of the modeled meteors that explain the observations at PFISR are within the 1–250 μg mass range while at Arecibo they are within 10^{-4}–10^{1} μg. This is in agreement with dynamical mass estimates derived from both systems, which suggests that PFISR's detected meteor rates are dominated by particles with masses 1–2 orders of magnitude larger than Arecibo (Janches et al., 2000; Sparks et al., 2008).

The modeled minimum electron volume density of $1 \times 10^{14}\,e^{-}/m^{3}$ used to model the sensitivity threshold of PFISR is significantly larger than the $1 \times 10^{8}\,e^{-}/m^{3}$ used to model Arecibo's (Fentzke and Janches, 2008). This requires that the larger particles observed by PFISR need to penetrate lower into the MLT in order to reach this threshold as the observations presented in a companion paper show (Sparks et al., 2008). Future versions of the model will include a rigorous treatment of the meteor RCS. This future modeling effort, which includes the parameterization of FDTD simulations of electromagnetic waves interacting with the head-echo plasma, is under current

development (Dyrud et al., 2007; Dyrud and Janches, 2008). However, the results presented here show that we can satisfactorily model the largely variable meteoric input into the MLT once the correct interpretation of instrument response function is applied.

Acknowledgments

The PFISR is operated by SRI International under NSF ATM-0608577 cooperative agreement. The Arecibo Observatory is part of the National Astronomy and Ionosphere Center, which is operated by Cornell University under cooperative agreement with the National Science Foundation. Also, the authors wish to thank Naomi Edelberg for her help on the analysis of the AO meteor data and Dr. S. Close for discussions and assistance with the interpretation of her RCS model. This work was supported under NSF Grants ATM-05311464 and ATM-0525655 to NorthWest Research Associates, Inc. and agreement 51861-8406 between Cornell University and NWRA.

References

Baggaley, W., 2002. Radar observations. In: Murad, E., Williams, I. (Eds.), Meteors in the Earth's Atmosphere. Cambridge University Press, Cambridge, MA, pp. 123–148.

Bronshten, V., 1983. Physics of Meteoric Phenomena. d. Reidel Publishing Co.

Ceplecha, Z., Borovička, J., Elford, W., Revelle, D., Hawkes, R., Porubčan, V., Šimek, M., 1998. Meteor phenomena and bodies. Space Science Reviews 84, 327–471.

Close, S., Oppenheim, M., Durand, D., Dyrud, L., 2005. A new method for determining meteoroid mass from head echo data. Journal of Geophysical Research (Space Physics) 110 (A9), 9308.

Close, S., Brown, P., Campbell-Brown, M., Oppenheim, M., Colestock, P., 2007. Meteor head echo radar data: mass–velocity selection effects. Icarus 186, 547–556.

Dyrud, L.P., Wilson, D., Boerve, S., Trulsen, J., Pecseli, H., Close, S., Chen, C., Lee, Y., 2007. Plasma and electromagnetic simulations of meteor head echo radar reflections. Earth, Moon and Planets, 65.

Dyrud, L.P., Janches, D., 2008. Modeling the meteor head-echo using Arecibo observations. Journal of Atmospheric Solar-Terrestrial Physics, this issue, doi:10.1016/j.jastp.2008.06.016.

Fentzke, J.T., Janches, D., 2008. A semi-empirical model of the contribution from sporadic meteoroid sources on the meteor input function observed at arecibo. Journal of Geophysical Research (Space Physics) 113 (A03304).

Galligan, D., Baggaley, W., 2005. The radiant distribution of amor radar meteors. Monthly Notices of the Royal Astronomical Society 359 (2), 551–560.

Hunten, D.M., Turco, R.P., Toon, O.B., 1980. Smoke and dust particles of meteoric origin in the mesosphere and stratosphere. Journal of Atmospheric Sciences 37, 1342–1357.

Janches, D., Chau, J., 2005. Observed diurnal and seasonal behavior of the micrometeor flux using the Arecibo and Jicamarca radars. Journal of Atmospheric and Solar-Terrestrial Physics 67, this issue, doi:10.1016/j.jastp.2005.06.011.

Janches, D., ReVelle, D., 2005. The initial altitude of the micrometeor phenomenon: comparison between arecibo radar observations and theory. Journal of Geophysical Research 110.

Janches, D., Mathews, J., Meisel, D., Zhou, Q., 2000. Micrometeor observations using the arecibo 430 MHz radar: I. determination of the ballistic parameter from measured doppler velocity and deceleration results. Icarus 145, 53–63.

Janches, D., Nolan, M., Meisel, D., Mathews, J., Zhou, Q., Moser, D., 2003. On the geocentric micrometeor velocity distribution. Journal of Geophysical Research 108 (A6), 1222.

Janches, D., Nolan, M., Sulzer, M., 2004a. Radiant measurement accuracy of micrometeors detected by the arecibo 430 MHz dual-beam radar. Atmospheric Chemistry and Physics 4, 621–626.

Janches, D., Palo, S., Lau, S., Avery, J., Avery, S., de la Peña, S., Makarov, N., 2004b. Diurnal and seasonal variability of the meteoric flux at the south pole measured with radars. Geophysical Research Letters 31.

Janches, D., Heinselman, C., Chau, J., Chandran, A., Woodman, R., 2006. Modeling the global micrometeor input function in the upper atmosphere observed by high power and large aperture radars. Journal of Geophysical Research 111.

Janches, D., Fritts, D., Nicolls, M., Heinselman, C., 2008. Observations of D-region structure and atmospheric tides with PFISR during active auror. Journal of Atmospheric and Solar-Terrestrial Physics, accepted.

Jones, J., Brown, P., 1993. Sporadic meteor radiant distribution: orbital survey results. Monthly Notices of the Royal Astronomical Society 265, 524–532.

Love, S.G., Brownlee, D.E., 1991. Heating and thermal transformation of micrometeoroids entering the earth's atmosphere. Icarus 89, 26–43.

McKinley, D.W.R., 1961. Meteor Science and Engineering. McGraw Hill, New York.

McNeil, W., Lai, S., Murad, E., 1998. Differential ablation of cosmic dust and implications for the relative abundances of atmospheric metals. Journal of Geophysical Research 103 (D9), 10899–10911.

McNeil, W., Murad, E., Plane, J., 2002. Models of meteoric metals in the atmosphere. In: Murad, E., Williams, I. (Eds.), Meteors in the Earth's Atmosphere. University Press, Cambridge, pp. 265–287.

McNeil, W.J., Murad, E., Lai, S.T., 1995. Comprehensive model for the atmospheric sodium layer. Journal of Geophysical Research 100, 16847–16856.

Megner, L., Rapp, M., Gumbel, J., 2006. Distribution of meteoric smoke—sensitivity to microphysical properties and atmospheric conditions. Atmospheric Chemistry and Physics 6, 4415–4426.

Pesnell, W., Grebowsky, J.M., Weisman, A.L., 2004. Watching meteors on triton. Icarus 169, 482–491.

Plane, J., 2004. A new time-resolved model for the mesospheric na layer: constraints on the meteor input function. Atmospheric Chemistry and Physics 4, 39–69.

Plane, J.M.C., 1991. The chemistry of meteoric metals in the upper atmosphere. International Reviews of Physical Chemistry 10, 55–106.

Singer, W., Weiß, J., von Zahn, U., 2004. Diurnal and annual variations of meteor rates at the Arctic circle. Atmospheric Chemistry and Physics 4, 1–20.

Sparks, J.J., Janches, D., Nicolls, M.J., Heinselman, C.J., 2008. Seasonal and diurnal variability of the meteor flux at high latitudes observed using PFISR. Journal of Atmospheric Solar-Terrestrial Physics, this issue, doi:10.1016/j.jastp.2008.08.009.

Taylor, A., 1997. Radiant distribution of meteoroids encountering the earth. Advances in Space Research 20 (8), 1505–1508.

Taylor, A., Elford, W., 1998. Meteoroid orbital element distribution at 1 au deduced from the harvard radio meteor project observations. Earth Planets and Space 50, 569–575.

Westman, A., Wannberg, G., Pellinen-Wannberg, A., 2004. Meteor head echo altitude distributions and the height cutoff effect studied with the EISCAT HPLA UHF and VHF radars. Annales Geophysicae 22, 1575–1584.

Whipple, F., 1950. The theory of micro-meteorites, part i: in an isothermal atmosphere. Proceedings of the National Academy of Sciences of the United States of America 36, 687–695.

Whipple, F., 1951. The theory of micro-meteorites, part ii: in an heterothermal atmospheres. Proceedings of the National Academy of Sciences of the United States of America 37, 19–30.

Williams, I.P., Murad, E., 2002. Introduction. In: Murad, E., Williams, I.P. (Eds.), Meteors in the Earth's Atmosphere. Cambridge University Press, Cambridge, MA, pp. 1–10.